Atropisomerism of phosphorus-containing *N*-aryl carbamates. Experimental and computational data

Yu. G. Gololobov,[a]★ V. I. Galkin,[b] P. V. Petrovskii,[a] O. A. Linchenko,[a] E. M. Zueva,[b] L. G. Mubarakova,[b] R. A. Cherkasov,[b] R. Schmutzler,[c] L. Ernst,[c] P. G. Jones,[c] and M. Freytag[c]

[a]*A. N. Nesmeyanov Institute of Organoelement Compounds, Russian Academy of Sciences, 28 ul. Vavilova, 119991 Moscow, Russian Federation. E-mail: Yugol@ineos.ac.ru*

[b]*Kazan State University, 18 ul. Kremlevskaya, 420008 Kazan, Russian Federation*

[c]*Institute of Inorganic and Analytical Chemistry, Technical University of Braunschweig, Postfach 3329, D-38023 Braunschweig, Germany.* E-mail: r.schmutzler@tu-bs.de*

Studies by ^{1}H NMR spectroscopy and X-ray diffraction analysis revealed hindered rotation of the aromatic substituent about the C_{Ar}—N bond in *ortho*-substituted (except for *o*-fluorine-substituted) phosphorus-containing carbamates. The energy barriers to rotation ($\Delta G_c^{\neq}$) and coalescence temperatures (T_c) determined by the coalescence method increase with increasing volume of the *ortho* substituent. Conformations resulting from rotation of the *ortho*-substituted aryl group about the C_{Ar}—N bond were analyzed by quantum-chemical methods, potential curves were constructed, and differences between the conformational energies and the heights of rotation barriers were estimated. The theoretical rotation barriers change in parallel with the experimental values of $\Delta G_c^{\neq}$; however, the theoretical values are much smaller in magnitude.

Key words: atropisomerism, *ortho* effect, X-ray diffraction analysis, phosphorus-containing carbamates, low-temperature NMR spectroscopy, quantum-chemical calculations.

The reactions of *ortho*-substituted aryl isocyanates with phosphorus-containing zwitterion **1** (Scheme 1), which was generated by the reaction of triisopropylphosphine with ethyl 2-cyanoacrylate,[1] were accompanied by the C→N migration of the ethoxycarbonyl group in the second step of the reaction to give phosphorus-containing carbamates **3**, **4**,[2] and **5**.

According to the ^{31}P NMR spectroscopic data, the insertion of isocyanates into the C—C bond of zwitterion **1** in the reactions with *ortho*-substituted aryl isocyanates (except for *o*-fluorophenyl isocyanate) proceeded more slowly compared to the reaction with phenyl isocyanate. The larger the *ortho* substituent (both as the electron donor and acceptor) in aryl isocyanate, the slower the formation of carbamates **3**. A serious hindrance to the formation of carbamates **3** is created by the *ortho*-substituent of the aromatic ring, apparently, in the second step of the reaction, which involves the nucleophilic substitution at the C atom of the ethoxycarbonyl group of intermediate **2**.[3] Consequently, one would expect the presence of short contacts between the *ortho* substituents in carbamates **3** and the ester and/or acetyl groups.

This overcrowding in the region of the *N*-aromatic substituent can lead to hindered rotation about the N—C_{Ar} bond and, as a consequence, to the appearance of chirality. Figure 1 shows the difference in the environment about the protons of the CH_2 and Me_2C groups for the enantiomers of compounds **3**. Thus, the *ortho* substituent in the aromatic ring of one enantiomer is located above the plane of Fig. 1, whereas this substituent in another enantiomer is located below the plane of this figure.

The enantiomeric asymmetry is evidenced by the data from ^{1}H NMR spectroscopy. In chiral molecules **3**, the protons of the CH_2 or Me_2C groups are in different environments (see Fig. 1) and, consequently, are diastereotopic. At the same time, hindered rotation would not be expected to be reflected in the multiplicities of the signals for the methyl protons of the *o*-tolyl and ethoxycarbonyl groups as well as of the signals for the phenyl and methine protons. These characteristic features are actually observed in the ^{1}H NMR spectra of carbamates **3** and **4** (except for carbamates **3** with X = H or F), the above-described characteristic features of the ^{1}H NMR spectra being observed already at ~20 °C for the compounds, which con-

* Institut für Anorganische und Analytische Chemie der Technischen Universität, Postfach 3329, D-38023 Braunschweig, Germany.

Published in Russian in *Izvestiya Akademii Nauk. Seriya Khimicheskaya,* No. 9, pp. 1820—1826, September, 2003.

1066-5285/03/5209-1920 $25.00

Scheme 1

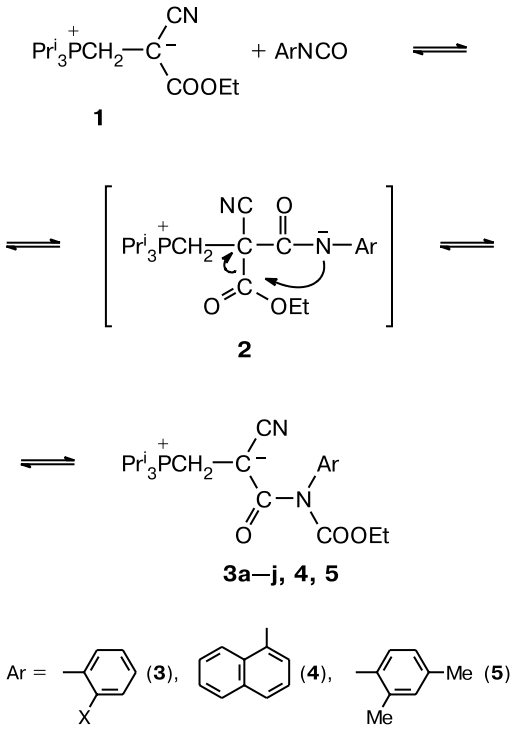

3: X = F (**a**), Cl (**b**), Br (**c**), I (**d**), Me (**e**), Et (**f**), Pr^i (**g**), Ph (**h**), MeO (**i**), CF_3 (**j**)

tain the *ortho*-substituents X with a volume of larger than 0.55* according to Charton[4] (compounds **3d,f,g,j** and **4**). The diastereotopism of the methylene and methyl protons of the isopropyl group in compounds **3b,e** is observed at temperatures below 20 °C. The diastereotopism of the methylene protons and the protons of the Me_2C groups in *o*-fluorophenyl derivative **3a** is not observed at all down to −70 °C. It should be noted that the larger the volume of the *ortho* substituent and the lower the temperature of measurements, the more pronounced the diastereotopic multiplicity of the protons of the CH_2 and Me_2C groups in the ^{1}H NMR spectra.

It should be emphasized that an increase in complexity of the spectra of the above-mentioned compounds is typical only of the methylene and methyl protons of the isopropyl groups at the P atom (in compound **3g**, the protons of the methyl groups of the isopropyl substituent in the *ortho* position of the phenyl ring are also diastereotopic). The multiplicities of the signals for the remaining protons as well as the multiplicity of the signal for the P atom (singlet) remain unchanged in the temperature range under consideration (down to −50 °C). At lower temperatures, the ^{1}H NMR spectra of compounds **3** become even more complex and require special analysis, which is beyond the scope of the present study.

* On this scale, the volume of the H atom is taken as zero.

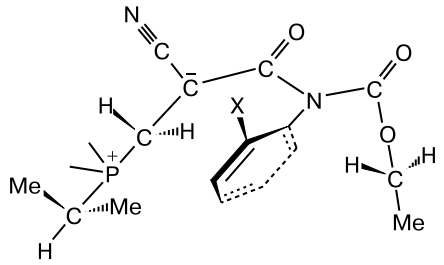

Fig. 1. Schematic representation of carbamates **3** in which the methylene protons, the methyl groups of the Pr^i—P fragment, and the methyl groups of the isopropyl fragment (X = Pr^i) are diastereotopic due to the presence of the *ortho*-substituted aryl ring.

The ^{1}H NMR spectrum of *o*-tolyl carbamate **3e** at ~20 °C displays signals with the expected multiplicities, *viz.*, a doublet of the CH_2P group and a quadruplet for the protons of the CH_2O group. However, the signals for the protons of the methylene group at the P atom are observed as a multiplet characteristic of an AB portion of an ABX spin system (X = P) at lower temperatures (this phenomenon is particularly pronounced at −40 °C). This fact indicates that the protons become nonequivalent as the temperature is decreased. By contrast, the ^{1}H NMR spectra of compound **3e** at low temperatures show only one signal for the *o*-methyl group, one triplet for the methyl group of the ethoxy fragment, and the characteristic multiplet for the methine proton. All these facts are evidence for asymmetry of molecule **3e** resulting from the hindrance to rotation of the *o*-tolyl fragment about the C_{Ar}—N bond. This assumption is in agreement with the X-ray diffraction data for carbamate **3e** (see below).

Analogous changes in the ^{1}H NMR spectra are observed also for other carbamates **3**. In the spectrum of carbamate **4** containing the 1-naphthyl substituent at the amide N atom, the nonequivalence of the protons of the CH_2P, CH_2O, and Me_2C groups is observed already at ~20 °C. However, this nonequivalence disappears upon heating of compound **4** in $CDCl_3$ to +55 °C, which is evidence that free rotation about the N—C_{Ar} bond in compound **4** is achieved at 55 °C, whereas this rotation is hindered at ~20 °C. Due to steric hindrance, the naphthyl ring deviates from the plane of the amidocarbamate groups giving rise to enantiomeric isomerism.

Earlier, the effect of hindered rotation of the 1-naphthyl group in carbamate structures has been observed by NMR spectroscopy for compound **4**,[5] a derivative of pyridinium ylide,[6] and purely organic compounds.[7]

The reasons for the hindrance to rotation of the *o*-tolyl, *o*-ethylphenyl, and 1-naphthyl substituents about the N—C_{Ar} bond can be understood from the X-ray diffraction data for compounds **3e,f** and **4** (Figs. 2—4). The principal crystallographic characteristics and geometric parameters of these compounds determined by X-ray dif-

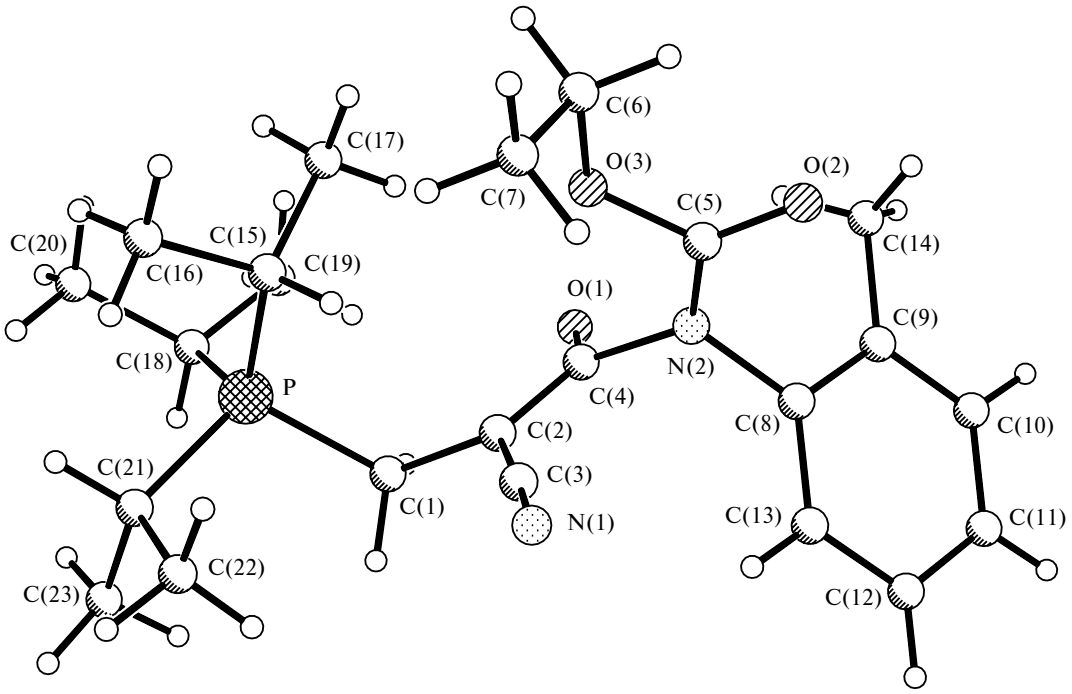

Fig. 2. Overall view and the atomic numbering scheme in zwitterion **3e** according to the results of X-ray diffraction study.

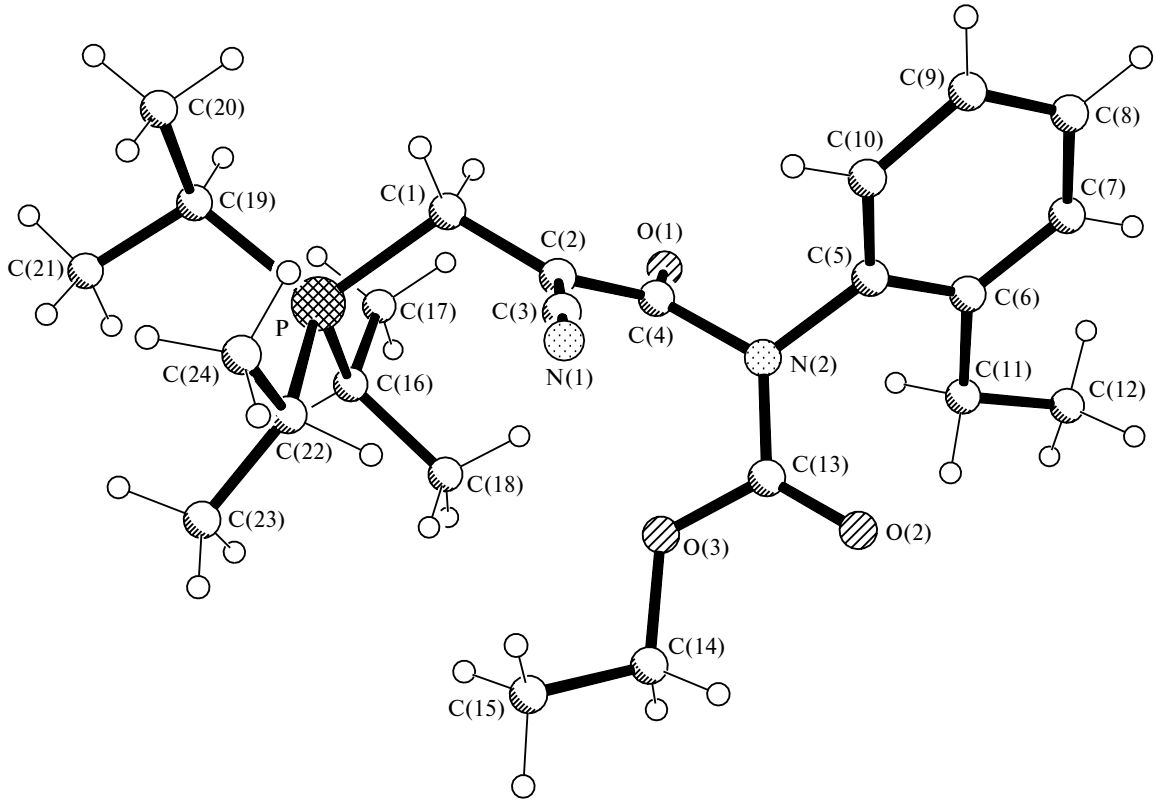

Fig. 3. Overall view and the atomic numbering scheme in zwitterion **3f** according to the results of X-ray diffraction study.

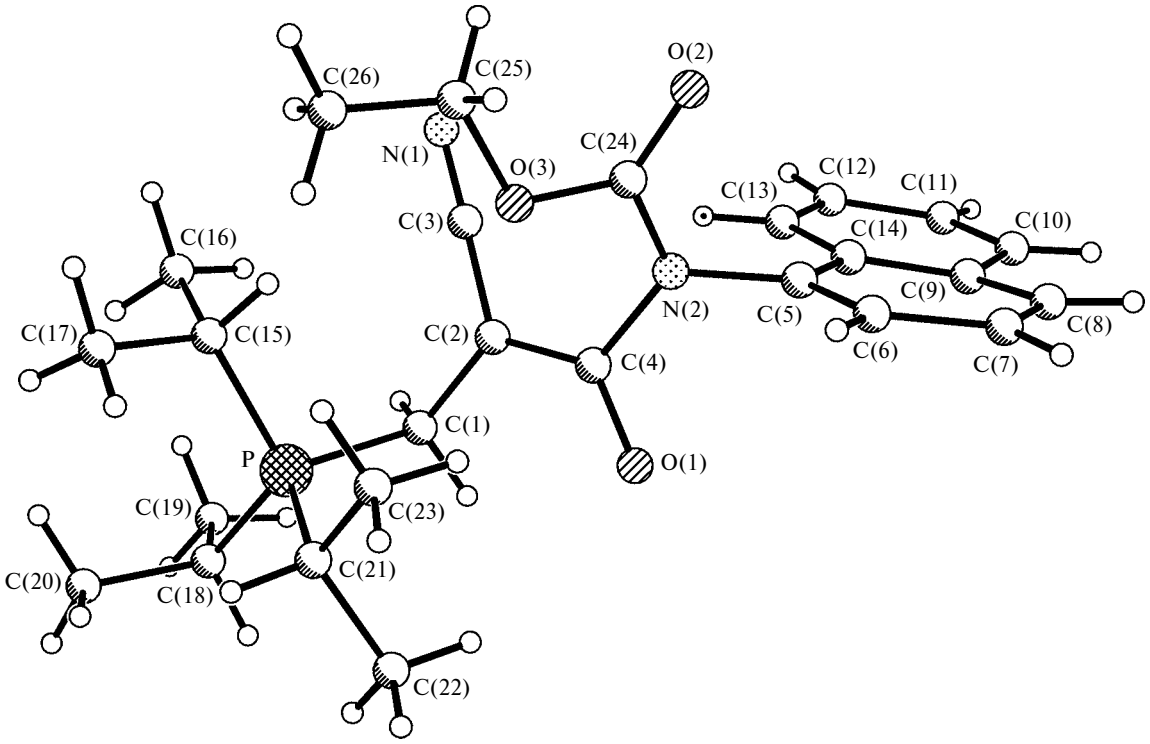

Fig. 4. Overall view and the atomic numbering scheme in zwitterion **4** according to the results of X-ray diffraction study.

Table 1. Crystallographic data for compounds **3e,f** and **4**

Parameter	**3e**	**3f**	**4**
Molecular formula	$C_{23}H_{35}N_2O_3P$	$C_{24}H_{37}N_2O_3P$	$C_{26}H_{35}N_2O_3P$
Molecular weight	418.50	432.53	454.53
Color, habitus	Colorless plates	Colorless needles	Colorless prisms
Crystal dimensions/mm	0.20×0.17×0.03	0.47×0.17×0.13	0.27×0.18×0.17
Temperature/°C	−130	−130	−130
Crystal system	Monoclinic	Tetragonal	Monoclinic
Space group	$P2_1/n$	I-4	$P2_1/c$
a/pm	1333.83(14)	3649.7(3)	768.99(10)
b/pm	2279.3(2)	3649.7(3)	1363.61(16)
c/pm	1515.97(14)	766.78(8)	2314.2(3)
α/deg	90	90	90
β/deg	97.621(6)	90	93.96(7)
γ/deg	90	90	90
U/nm^3	4.5682(8)	10.2136(15)	2.4209(5)
Z	8	16	4
d_{calc}/Mg m^{-3}	1.217	1.125	1.247
μ/mm^{-1}	0.146	0.132	0.143
F(000)	1808	3744	976
$2\theta_{max}$/deg	50	52	52
Number of measured reflections	51699	57310	29514
Number of independent reflections	8059	10459	4961
R_{int}	0.1500	0.0857	0.0992
$wR(F^2)$ (all reflections)	0.1800	0.1327	0.1386
$R(F > 4\sigma(F))$	0.0747	0.0485	0.0540
Number of parameters	612	566	395
GOOF	1.028	1.052	1.026

Table 2. Selected bond lengths (*d*) and bond angles (ω) in compounds **3e,f** and **4**

Parameter	3e	3f	4
Bond		*d*/Å	
P—C(1)	1.821(4)	1.825(3)	1.823(3)
C(1)—C(2)	1.506(5)	1.509(3)	1.502(3)
C(2)—C(4)	1.382(5)	1.390(3)	1.386(3)
C(4)—N(2)	1.468(5)	1.468(5)	—
C(4)—O(1)	1.245(5)	1.236(3)	1.239(3)
C(2)—C(3)	1.420(6)	1.410(3)	1.418(3)
C(3)—N(1)	1.150(5)	1.162(3)	1.158(3)
Angle		ω/deg	
P—C(1)—C(2)	117.2(3)	116.9(19)	116.9(16)
C(1)—C(2)—C(4)	119.2(4)	121.1(2)	121.0(2)
C(2)—C(4)—N(2)	116.3(4)	115.4(2)	—
C(4)—N(2)—C(5)	124.9(3)	124.7(2)	—

fraction analysis are given in Tables 1 and 2, respectively. It is noteworthy that the protons of the *o*-methyl or *o*-ethyl group as well as the *peri*-proton of the naphthyl fragment form short contacts with the carbonyl oxygen atom of the ethoxycarbonyl group. These contacts are comparable to the sum of the van der Waals radii of the proton and the O atom (2.6 Å). In the crystal, the shortest distances from the carbonyl oxygen atom of the C(O)OEt group to the protons of the *o*-methyl or *o*-ethyl group and to the *peri*-proton of the 1-naphthyl fragment are 2.73, 2.45, and ~3.0 Å, respectively. Evidently, it is these steric factors that are responsible for hindrance to rotation of the above-mentioned aryl groups about the N—C_{Ar} bond resulting in enantiomeric isomerism of the corresponding carbamates.

The energy barriers to rotation ($\Delta G_c^{\neq}$) characterizing the hindrance to rotation about the N—C_{Ar} bond in compounds **3a—d,f,h**, **4**, and **5** were determined by the coalescence method[8—10] (Table 3).

In the $^1H\{^{31}P\}$ NMR spectra of all the compounds (except for **3a**) listed in Table 3, which were measured with proton decoupling, the signal for the protons of the CH_2P group decoalesces into an AB quartet at the indicated coalescence temperature (T_c). The *o*-fluoro- and *o*-chlorophenyl substituents are most readily rotated about the C—N bond. For derivatives **3a** and **3b**, hindrance to rotation of the aryl fragment is not observed down to −75 and −19 °C, respectively. The ethyl substituent in the *ortho* position (compound **3f**) creates the largest hindrance to rotation. We failed to determine $\Delta G_c^{\neq}$ and, correspondingly, T_c for compound **3g** because the latter decomposed upon heating to 100 °C in a solution in CCl_2DCCl_2D.

The temperature dependence of the $^1H\{^{31}P\}$ NMR spectrum of iodine-containing derivative **3d** presented in Fig. 5 shows that the signals for the protons of the CH_2P group are transformed into a singlet at ~50 °C and into an AB quartet at $T < +20$ °C ($T_c = +25$ °C). These data are

Table 3. Energy barriers to rotation ($\Delta G_c^{\neq}$) and coalescence temperatures (T_c) according to the ^1H NMR spectroscopic data for compounds **3a—d,f,h**, **4**, and **5**

Compound	X	*r*[a] /Å	$\Delta G_c^{\neq}$ /kJ mol^{-1}	T_c /°C	Δν[b] /Hz
3a	F	1.35	<40.0	<−75	45[c]
3b	Cl	1.80	51.7±0.8	−19±3	42±5
3c	Br	1.95	56.6±0.9	4.5±3	45±8
3d	I	2.15	60.9±0.9	25±1.5	48±8
3f	Et	—	62.9±1.0	32.2±3	30±10
3h	Ph	1.70	53.0±1.2	−2±5	153±10
4	—	—	63.0±1.0	32±4	29±2
5	Me[d]	2.00	56.1±0.9	0±3	27.8±5

[a] The covalent radius of the substituent X.
[b] The difference between the chemical shifts of the protons of the CH_2P group in the $^1H\{^{31}P\}$ NMR spectrum at T_c.
[c] The estimated value.
[d] The compound contains also the methyl group in the *para* position.

indicative of slow rotation of the *o*-iodine-substituted aryl ring about the N—C_{Ar} bond at ~20 °C. At low temperature, steric hindrances are responsible for deviation of this ring from the plane of the acylcarbamate group due to which the protons of the CH_2P group become diastereotopic.

A correlation of the volume characteristics of the substituents X with the values of $\Delta G_c^{\neq}$ demonstrated (see Table 3) that the latter increase as the volume of the *ortho*-substituent increases. The energy barrier to rotation for *o*-tolyl derivative **3e** is intermediate between the characteristics for the *o*-chloro and *o*-bromo derivatives and is closer to the latter value. Evidently, decoalescence of the signal for the protons of the CH_2P group in derivative **3a** was not observed down to −75 °C due to a small size of the F atom. Calculations based on Δν for halide-containing derivatives **3b—d** led to the conclusion that $\Delta G_c^{\neq}$ for **3a** should not be higher than 40.0 kJ mol^{-1} (9.5 kcal mol^{-1}) at this temperature.

As a continuation of our studies, it was of interest to compare the experimental energy barriers to rotation $\Delta G_c^{\neq}$ of the *ortho*-substituted aryl substituents about the N—C_{Ar} bond and correlate the conclusions made based on these data with the results of quantum-chemical calculations. For this purpose, we carried out quantum-chemical calculations for **6a—c,f,h,j** and **7**, which completely model the above-described compounds **3a—c,f,h,j** and **4**, respectively. Model structures **6** and **7** differ from real compounds **3** and **4** only in that the isopropyl groups at the P atom in the latter compounds are replaced by the methyl groups to simplify quantum-chemical calculations.

For these structures (**6a—c,f,h,j**, **7**), the conformations resulting from rotation about the N—C_{Ar} bond were analyzed, potential curves were constructed, the differ-

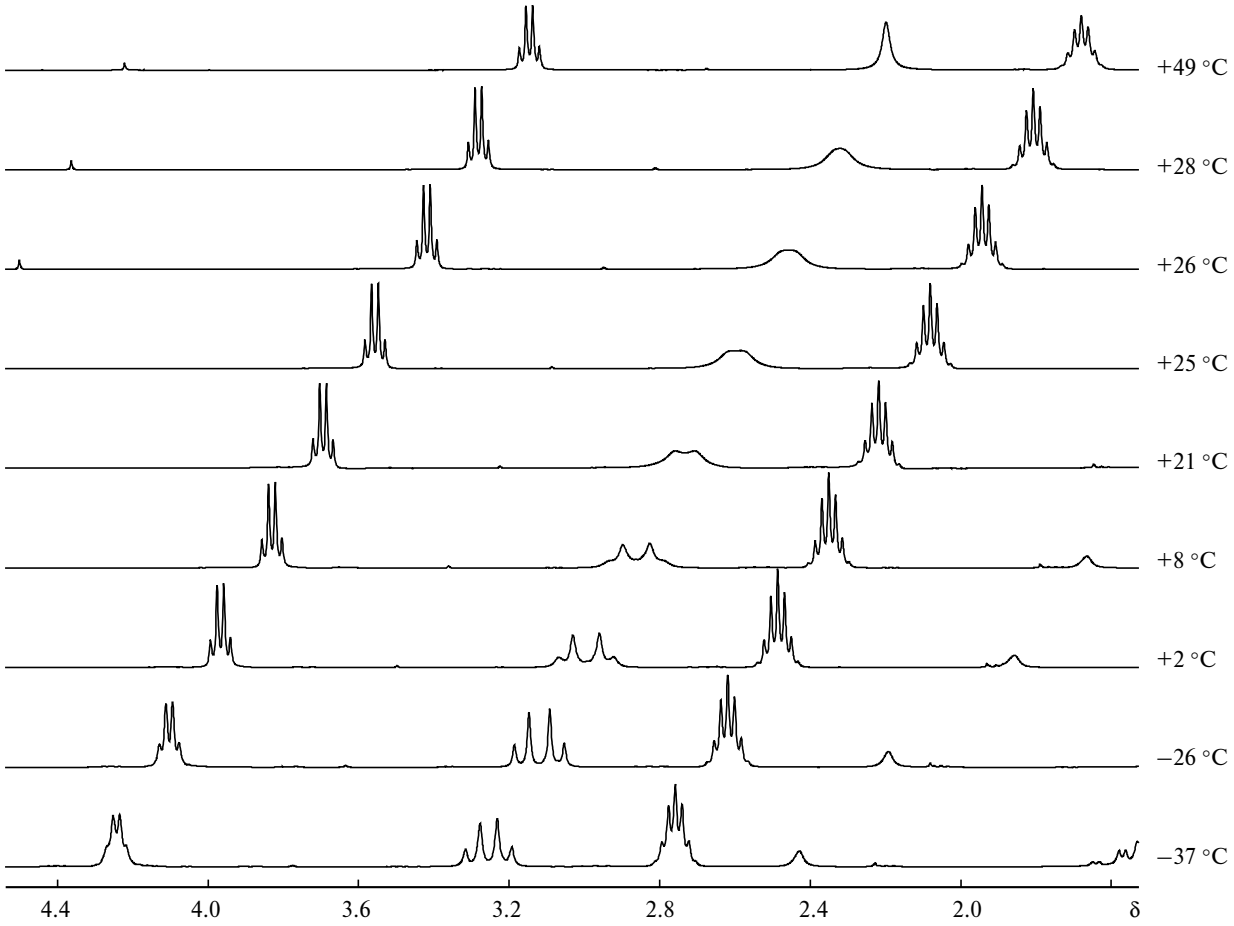

Fig. 5. Temperature dependence of the signals in the $^1H\{^{31}P\}$ NMR spectrum of compound **3d**.

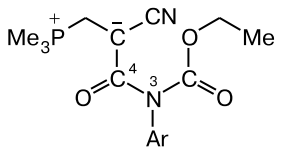

6a—c,f,h,j, 7

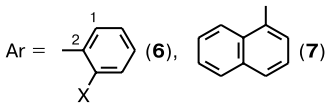

6: X = F (**a**), Cl (**b**), Br (**c**), Et (**f**), Ph (**h**), CF_3 (**j**)

ences between the conformational energies were estimated, and the rotation barriers were evaluated. The C(1)—C(2)—N(3)—C(4) torsion angle (φ) was chosen as the reaction coordinate. The OEt fragment was specified so that the O—C and C=O bonds are in *cis* positions with respect to each other and the least eclipsed conformation of all possible conformations resulting from rotation about the Me_3P^+C—C bond was considered. Table 4 lists the total energies (E_{tot}) corresponding to the maxima and minima in the potential curves for the compounds under study at the given torsion angles φ. As an example, the potential curves for molecules **6c** and **7** constructed by the semiempirical AM1 method are shown in Fig. 6, *a*, *b*. The barriers to rotation (ΔE) are given in Table 5.

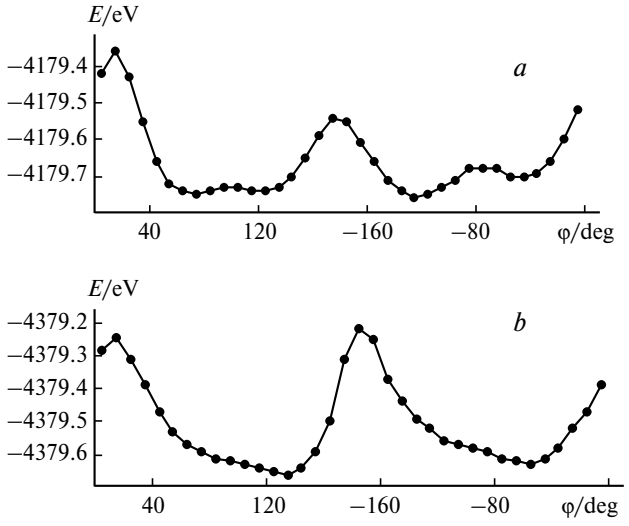

Fig. 6. Potential curves of rotation about the N—C_{Ar} bond in compounds **6c** (*a*) and **7** (*b*).

Table 4. Total energies (E_{tot}) corresponding to the maxima (max) and minima (min) in the potential curves for the compounds under study at the given C(1)—C(2)—N(3)—C(4) torsion angles (φ)

Compound	φ/deg	$-E_{tot}$/eV
6a	0	4311.591 (max 1)
	40	4311.731 (min 1)
	180	4311.540 (max 2)
	−70	4311.733 (min 2)
6b	0	4199.992 (max 1)
	50	4200.286 (min 1)
	170	4200.117 (max 2)
	−130	4200.300 (min 2)
6c	5	4179.367 (max 1)
	60	4179.748 (min 1)
	170	4179.535 (max 2)
	−130	4179.759 (min 2)
6f	8	4151.529 (max 1)
	90	4151.804 (min 1)
	180	4151.533 (max 2)
	−50	4151.823 (min 2)
6h	0	4662.087 (max 1)
	50	4662.588 (min 1)
	180	4661.441 (max 2)
	−70	4662.716 (min 2)
6j	180	5410.385 (max 1)
	60	5410.743 (min 1)
	−5	5410.508 (max 2)
	−80	5410.765 (min 2)
7	5	4379.245 (max 1)
	130	4379.593 (min 1)
	175	4379.247 (max 2)
	−60	4379.558 (min 2)

Table 5. Lowest rotation barriers (ΔE) for molecules **6a—c,f,h,j** and **7**

Compound	ΔE /kJ mol^{-1}	Compound	ΔE /kJ mol^{-1}
6a	13.3	**6h**	60.6
6b	17.5	**6j**	24.6
6c	21.3	**7**	37.6
6f	28.0		

Our calculations demonstrated that the potential curves for all the compounds under consideration have two flat maxima. The structures corresponding to the maxima and minima in this curve are bipolar ions in which the interaction between the P^+ and C^- centers can be qualitatively described as a nonbonded attractive n—σ*-type interaction. Sterically uncrowded structures in which there is no conjugation between the N atom and the aromatic system correspond to stable conformations of the molecules under consideration. In all structures, the N atom has an almost planar configuration (the sum of the bond angles is in the range of 352—360°). The O=C—C—CN fragment is also planar. These geometric features are in good agreement with the above-described results of X-ray diffraction study of compounds **3e,f** and **4**, which indicates that the geometry of the molecules is adequately reproduced by the chosen quantum-chemical method. The lowest potential barrier calculated from the most favorable conformation is controlled by steric interactions between the substituent X and the carbonyl groups at the N atom (see Table 5). The energy barrier to rotation of the *ortho*-substituted aromatic fragment about the C_{Ar}—N bond (see Table 5) increases as the volume of the *ortho*-substituent increases. The experimental data are in qualitative agreement with the results of quantum-chemical calculations. The quantitative discrepancy between the calculated and experimental parameters arises, apparently, from the assumed model approximations and the effect of the solvent because calculations were carried out for the gas phase.

Therefore, the C→N migration of the alkoxycarbonyl groups, which we have found earlier and applied[2] to the preparation of *ortho*-substituted carbamates **3**, allowed us to reveal and quantitatively study hindered rotation of the aromatic substituent about the single C—N bond in organophosphorus zwitterions.

Experimental

The synthesis of compounds **3a—j**, **4**, and **5** was described by us earlier.[2] The NMR spectra were measured on a Bruker DRX-400 spectrometer (at 400.1 MHz for ^{1}H, 100.6 MHz for ^{13}C, and 162.0 MHz for ^{31}P). Low-temperature measurements were carried out using a Bruker VT-3300 unit ($CDCl_3$ or CD_2Cl_2 as the solvents). Low temperatures were controlled by "an NMR thermometer" using a standard solution of methanol in CD_3OD. Temperatures higher than 20 °C were controlled by "an NMR thermometer" using a standard solution of ethylene glycol in DMSO-d_6 (accuracy of determination was ±3 °C). To simplify the calculations for the CH_2P group, the variable-temperature $^1H\{^{31}P\}$ NMR spectra were recorded. Consequently, the signals for the protons of the CH_2P group were observed as a singlet at high temperatures and as an AB system at low temperatures. The rate constants (k_c) at coalescence temperatures T_c were calculated according to the equation $k_c = [(\Delta\nu)^2 + 6J_{AB}^2]^{0.5}$.[8] The differences between the chemical shifts ($\Delta\nu$) within the AB spectra were extrapolated to T_c. The free energy of rotation $\Delta G_c^{\neq}$ was determined according to the equation $\Delta G_c^{\neq}$/kJ mol^{-1} = $0.01914T_c[10.32 + \log(T_c/k_c)]$.[9] The signals with nonequivalent intensities were calculated using a known method,[10] which is strictly appropriate only for coalescent singlets. Therefore, the corresponding results should be considered as rough data.

X-ray diffraction study was carried out on a Bruker SMART 1000 CCD diffractometer equipped with a low-temperature LT-3 unit (Mo-Kα radiation, graphite monochromator). The structures were solved by direct methods and refined anisotropically

based on F^2 using the SHELXL-97 program package.[11] The geometric parameters of compounds **3e,f** and **4** are identical to those of the structurally analogous zwitterions considered earlier.[2] The crystallographic data for compounds **3e,f** and **4** are given in Table 1. Selected bond lengths and bond angles in these compounds are listed in Table 2. The complete tables of the bond lengths, bond angles, atomic coordinates, and thermal parameters were deposited with the Cambridge Structural Database.

Quantum-chemical calculations. Calculations were carried out by the AM1 quantum-chemical method using the MOPAC 7.0 program. The geometric parameters were optimized by the BFGS method, SCFCRT = 0.000001 kcal mol^{-1} (the SCF criterion, which is the difference between the energies in the n-th and $(n - 1)$-th iterations, should be smaller than SCFCRT).

This study was financially supported by the German Research Council (Deutsche Forschungsgemeinschaft, Grant 433 RUS 17/44/99).

References

1. Yu. G. Gololobov, G. D. Kolomnikova, and T. O. Krilova, *Tetrahedron Lett.*, 1994, **35**, 1751.
2. Yu. G. Gololobov, P. V. Petrovskii, E. M. Ivanova, O. A. Linchenko, R. Schmutzler, L. Ernst, P. G. Jones, A. Karaçar, M. Freytag, and S. Okucu, *Izv. Akad. Nauk, Ser. Khim.*, 2003, 409 [*Russ. Chem. Bull., Int. Ed.*, 2003, **52**, 427].
3. V. I. Galkin, Yu. V. Bakhtiyarova, Yu. Krasnova, Yu. G. Gololobov, N. A. Polezhaeva, and R. A. Cherkasov, *Heteroatom Chem.*, 1998, **9**, 665.
4. M. Charton, *J. Am. Chem. Soc.*, 1975, **97**, 369.
5. Yu. G. Gololobov, N. A. Kardanov, V. N. Khroustalyov, and P. V. Petrovskii, *Tetrahedron Lett.*, 1997, **38**, 7437.
6. Yu. G. Gololobov, O. V. Dovgan, P. V. Petrovskii, and I. A Garbusova, *Heteroatom Chem.*, 2002, **13**, 665.
7. S. Julià, A. Ginebreda, P. Sala, M. Sancho, R. Annunziata, and F. Cozzi, *Org. Magn. Reson.*, 1983, **21**, 573.
8. R. J. Kurland, M. B. Rubin, and W. B. Wise, *J. Chem. Phys.*, 1964, **40**, 2426.
9. H. Friebolin, *Basic One- and Two-Dimensional NMR Spectroscopy*, 3rd ed., Wiley—VCH, Weinheim, 1998, 309.
10. J. H. Muensch, H. G. Schmid, H. Friebolin, and A. Mannschreck, *J. Mol. Spectrosc.*, 1969, **31**, 14.
11. G. M. Sheldrick, *SHELXL-97. Program for Crystal Structure Refinement*, Universität Göttingen, Göttingen, 1997.

Received February 3, 2003;
in revised form June 3, 2003